




Original Paper

Anthropogenic Aquifer Recharge Effect on Groundwater Resources in an Agricultural Floodplain in Northeastern Tunisia: Insights from Geochemical Tracers and Geophysical Methods

Anis Chekirbane ^{1,5}, Omeyma Gasmi,² Ammar Mlayah,² Hakim Gabtni,² Samia Khadhar,² Fethi Lachaal,² Adel Zghibi,³ and Jean-Denis Taupin⁴

Received 2 August 2021; accepted 22 November 2021
Published online: 10 January 2022

In this study, geochemical tracers and geophysical methods were combined to assess the anthropogenic aquifer recharge (AAR) processes within a small floodplain in Mornag plain, NE of Tunisia. From a regional viewpoint, the aquifer is one of the most exploited because of the intensive agricultural and industrial activities in the region. Based on geochemical data and hydrodynamic observations, stream–aquifer connection was evidently proven. An AAR from the saline effluent rejected in the dry channel (the Wadi) was detected in the downstream area of the Wadi El Hma plain. Isotopic tracers (^{18}O and ^2H) were effective tools to clarify the recharge processes in relation to the hill dam to detect the signature of the effluent near an installed check dam. Electrical resistivity tomography (ERT) profiles were performed in the most salinized part of the plain in order to highlight the role of the Wadi in AAR. ERT provided clear images of low resistivity horizons longitudinally and transversely to the Wadi. Because groundwater is mainly used for irrigation in the Wadi El Hma plain, an assessment of its suitability for irrigation was performed based on a multi-criteria decision analysis, which revealed that, except the hill dam water and upstream groundwater, the remaining zones of the aquifer are providing water classified as doubtful to unsuitable for irrigation. The results of this work highlight the water sustainability threat in the region and would warn decision-makers to control the Wadi runoff and preserve it against any pollution source since it constitutes the principal inlet of any AAR.

KEY WORDS: Anthropogenic aquifer recharge, Geochemical tracers, ERT, Irrigation suitability index.

¹Department of Rural Engineering, Water and Forests, National Institute of Agronomy of Tunisia (INAT), University of Carthage, Tunis, Tunisia.

²Laboratory of Georesources, Water Research and Technologies Center, Borj Cedria Technopark, Sulayman, Tunisia.

³LR01ES06 Laboratory of Geological Resources and Environment, Department of Geology, Faculty of Sciences of Tunis, University of Tunis El Manar, Tunis–El Manar Campus, 2092 Tunis–El Manar, Tunisia.

⁴Hydrosociences Montpellier, UMR 5151, University of Montpellier, IRD, CNRS, 34090 Montpellier, France.

⁵To whom correspondence should be addressed; e-mail: a.chkirbane@ecopark.rnrt.tn

INTRODUCTION

Food production for consumption and export has tremendously increased over the last 50 years. This agricultural activity used more than 40% of irrigation in the world depending on groundwater resources (Godfray et al., 2010). The situation is more serious in arid and semiarid regions. In fact, these regions are unceasingly growing and including

more of the earth's land surface (Schlesinger et al., 1990) with an area of 30% (Dregne, 1991; Scanlon et al., 2006) and contain some of the most populated areas in the world (Brown et al., 2005). Water resources evolution scenarios predict a global water shortage in the horizon of 2050 with decreasing rainfall and limited groundwater recharge (Milly et al., 2005; Döll and Florke, 2005).

Sustainability is the strategic purpose of all water policies and management plans. As water demand is growing continuously with population increase, water availability has become a crucial concern. In addition, in vulnerable arid and semiarid areas, human populations and ecosystems are relying intensively on groundwater resources to satisfy their essential water needs. The combined effect is inevitably affecting groundwater sustainability through over-pumping of aquifers, lowering of groundwater table level and speeding up quality deterioration. These facts will in turn affect water availability and cause several environmental problems such as soil salinization, lower crop yield and ecosystem degradation (Schoups et al., 2006; Praveena et al., 2012; Vadiati et al., 2018) as well as socioeconomic difficulties (Mays, 2013).

In the last two decades, special care has been given to the growing interest in groundwater sustainability, especially under arid and semiarid climate. In fact, great effort has been devoted to various interpretations depending on whether groundwater reservoirs are irreversibly or permanently lost as a result of large pumping rates that lead to environmental and ecological damages (Custodio, 2002; Morsy et al., 2018; Ranjan, 2012). Groundwater recharge was also considered as a sustainability indicator (Healy & Cook, 2002; Scanlon et al., 2002; Gleason et al., 2012). However, several studies argued that natural recharge alone cannot orient policies toward sustainable groundwater resources management (Balleau, 2013). Instead, they considered that another component should be taken into consideration: anthropogenic aquifer recharge (AAR), which comprises incidental recharge as a result of human activities that unintentionally increases recharge (Maliva, 2020).

Many studies tried to assess the anthropogenic impacts on groundwater resources in arid and semiarid regions using diverse methods. Zume and Tarhule (2011) studied the impact of anthropogenic pumping and recharge variability on an alluvial aquifer in semiarid northwestern Oklahoma using numerical simulation. Leitão et al. (2013) used water

quality data with geoelectrical methods to assess the diffuse contamination of a karstic aquifer in Algarve region, Portugal. Li et al. (2019) tried to understand the hydrochemical evolution of groundwater in a regional aquifer system in Yinchuan plain in China as a result of anthropogenic activities using stable isotopes and major chemical elements. Singha et al. (2019) identified the groundwater zones that are affected by anthropogenic contaminants in Raipur District, central India, using multi-criteria decision analysis—analytical hierarchy process (MCDA–AHP) technique combined with spatial analysis (i.e., using GIS). Nonetheless, most of these studies have focused on regional groundwater flow systems; they barely investigated the impact of anthropogenic activities on groundwater resources from a local-scale viewpoint. Moreover, there is still a lack of interest in the use of an integrated approach based on a multi-discipline intersection to clarify the AAR processes in poorly monitored groundwater flow systems.

In Tunisia, where climate is dominantly arid and semiarid, the availability of shallow groundwater resources is linked usually to recharge abundance, which is related to the infiltration of rainwater. In addition, more than 40% of groundwater resources are over-used in agriculture, drinking water supply and industry (Frija et al., 2014). Consequently, a continuous decline was observed in most aquifers of Tunisia, which is associated usually with water quality deterioration (Closas et al., 2018). The Mornag aquifer, located in the northeast of Tunisia, constitutes a typical case of a stressed aquifer; it is pumped heavily to satisfy the socioeconomic development of one of the most productive provinces of Tunis. However, during the last two decades, groundwater in this region has been under several constraints related to quantity and quality. In fact, a water table drawdown of more than 10 m was noticed and associated with groundwater salinization of many parts of the aquifer (Jarraya–Horriche and Wolfgang, 2019). The plain of the Wadi El Hma constitutes the central part of the basin where a sudden increase in groundwater salinity was registered during the last 5 years. Most of the intensive agriculture activities are almost concentrated in this region. Thus, an aquifer sustainability problem is posed and needs to be understood and solved. To the authors' best knowledge, small-scale investigation of groundwater sustainability issues was not previously addressed in this region. AAR was not also studied, and the question of groundwater

salinization is still debated by the scientific and technical community dealing with the Mornag plain. Therefore, the objectives of the present work were to (a) understand the issues related to groundwater resources in a local scale along the Wadi El Hma flood plain, (b) clarify their recharge processes, (c) explain their salinity origins and (d) assess their suitability for irrigation use as principal assets toward aquifer sustainability in the region.

STUDY AREA

The El Hma floodplain is a part of the Mornag plain located in the junction between the governorates of Ben Arous, Nabeul and Zaghouan. With an area of $\sim 250 \text{ km}^2$, the Mornag plain is located in the northeastern part of Tunisia within latitudes $36^\circ 34'$ to $36^\circ 46'$ N and longitudes $10^\circ 6'$ to $10^\circ 24'$ E (Fig. 1). More precisely, this sector is limited to the NW by the lower plain of Mejerda, to the East by the Gulf of Tunis, to the SE by the Tunisian Dorsale which includes the mountains of Sidi Salem, Zaghouan, Ressas and Bougarnine, to the West by the hills of Rades, Megrine, Bir Kassâa and Tella mount and to the SW by the hills of Khelidia. The focus area is the El Hma floodplain, which is particularly standing on the piedmonts of Ressas and Majoura Mountains. It is characterized by a flat topography ranging between 11 and 30 m (a.m.s.l.) in its downstream part and exceeding 200 m (a.m.s.l.) in its upstream zone. From the climate viewpoint, the region belongs to the semiarid stage with a mean annual precipitation of 465 mm. The most humid month is December with a mean rainfall of 72 mm, and the least is July with mean precipitation less than 7 mm. The region is characterized by mild winter and hot and dry summer. The annual average temperature is $\sim 19.1^\circ \text{C}$, and the mean annual evaporation is 1700 mm/yr (INM, 2018).

The plain is principally drained by the El Hma River, a non-perennial channel with irregular runoff, usually so-called Wadi in arid and desertic regions of North Africa and Middle East. The upstream part of this Wadi lodges a hill dam (El Hma dam) with a capacity of 12.1 Mm^3 , used principally to secure irrigation water and secondary for rare artificial recharge of the aquifer throughout water releases during the humid periods. A check dam was built on the Wadi bed to reduce its water flow and enhance its infiltration (Fig. 1). The watershed of the Wadi El Hma is one of the most fertile zones of Tunisia and

Ben Arous provinces. It was famous for more than a century for vine, citrus, peach and olive tree orchards. However, since 2018, a sudden increase in groundwater salinity reaching more than 6 g/l was registered especially in the wells located in the vicinity of the Wadi El Hma and which was hindering crop yield in the neighboring farms. The El Hma watershed also includes some industrial activities, mainly a cement manufactory exploiting a limestone quarry located on the piedmont of the Ressas Mountain. Field investigation revealed that the factory was discharging its wastewater with a salinity of 16.5 g/l into the Wadi El Hma through a sewer pipe (Fig. 1). Mixed with the rare natural water runoff, this effluent may considerably affect the groundwater quality of the floodplain.

GEOLOGICAL AND HYDROGEOLOGICAL SETTINGS

The geological context of the Mornag plain has been the subject of several studies (Boutib, 1998; Bujalka et al., 1972; Farhat, 2011; Jauzein, 1967; Soussi et al., 2000; Turki, 1985). The region is considered as an alluvial plain where Neogene and Quaternary sediments significantly dominate. Continental and fluvial detrital formations result from the dismantling of the surrounding reliefs. From a lithostratigraphic point of view, the outcropping formations have ages ranging from Eocene to Quaternary with notable lateral variations in facies (Fig. 2). Triassic, Jurassic and Cretaceous outcrops are located at the surrounding mountains. The El Hma plain is composed dominantly of Quaternary deposits of silts, clays and sands. Quaternary formations are distributed heterogeneously in the plain, but their maximum thickness is roughly at the central part with depth exceeding 600 m (Farhat, 2011). The Wadi beds are formed by recent alluvial deposits.

In regional hydrogeological scale, the Mornag plain lodges a complex multilayered aquifer composed of Quaternary alluvial deposits and sandstone lenses of Miocene and Oligocene age (Ennabli, 1980; Farhat, 2011; Mamou, 1994; Merhebene, 1998). The shallow aquifer follows a syncline structure and lies in angular discordance on the Miocene and Oligocene Formations (Moussa et al., 2020). With estimated reserves of $18.7 \text{ Mm}^3/\text{yr}$ (Jarraya-Horriche, 2004), the unconfined unit is found usually at depths ranging between 10 and 45 m (Farhat,

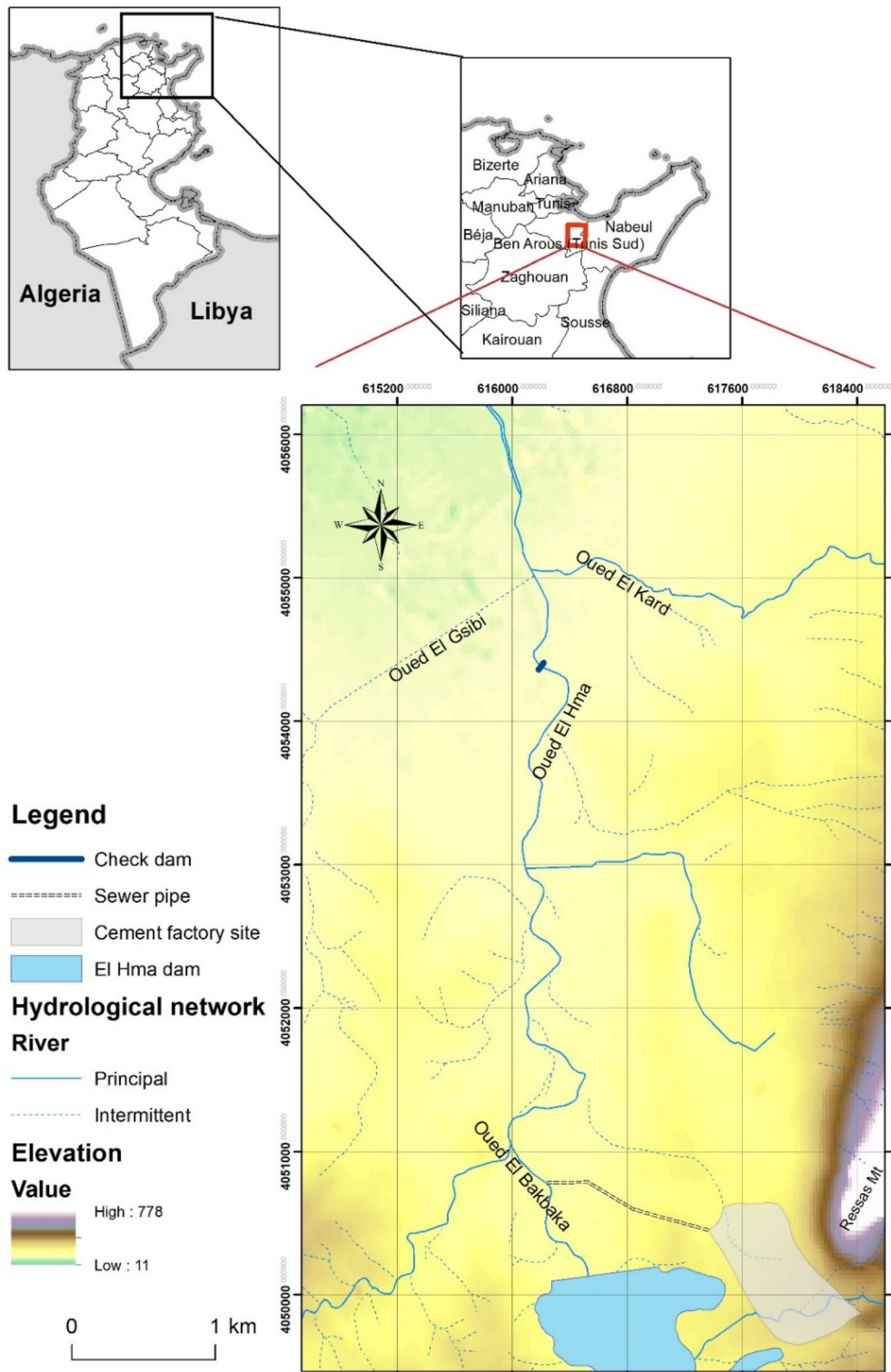


Figure 1. Study area location.

Geological outcrops

Age

- cQ: Mid-late Pleistocene
- aM3: Late Miocene
- M1-2: Late-medium Miocene
- M1; Aquitanien
- O: Early Oligocene
- aE2-3: Luthetien-Priabonien
- gE1: Ypresian
- Cm2-P: Eary Maestrichtien-Paleocene
- dC2: Late Senonian
- cdC2: Non subdivided Senonian
- cC2: Early Senonian
- VaC2: Vraconian Turonian
- sC1: Early Cretaceous
- J3: Malm
- J1-2: Lias-Dogger
- T: Trias

Hydrological network

River

- Principal
- Intermittent

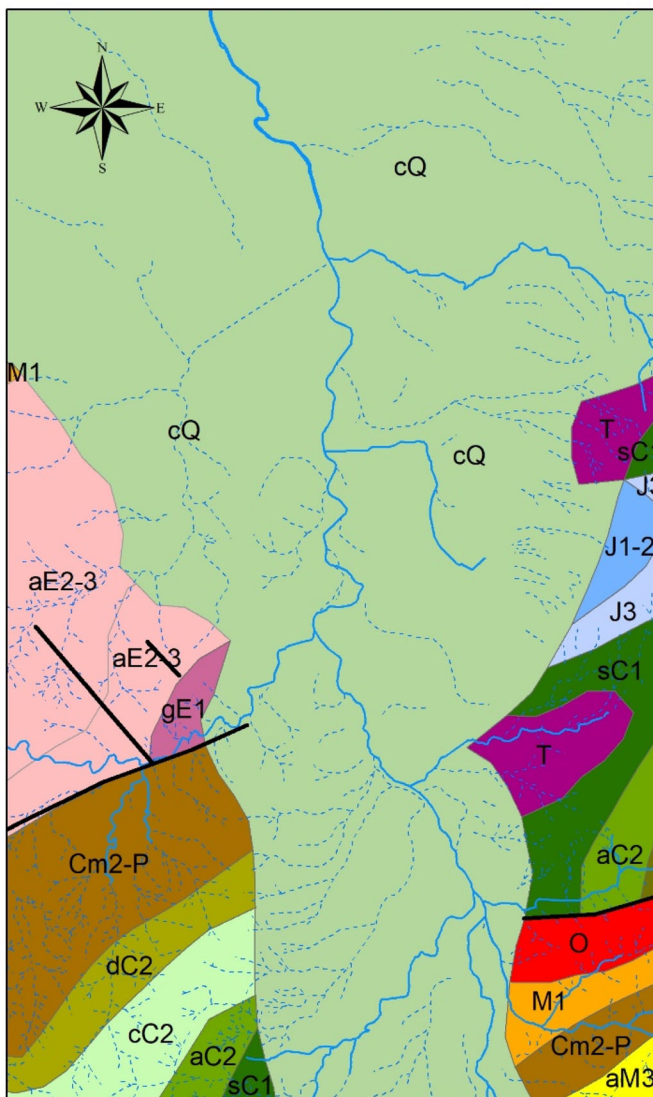
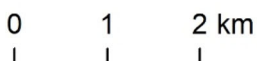


Figure 2. Geological map of the El Hma plain (from the 1:500 000 scale geological map of Tunisia, Ben Haj Ali et al. (1985)).

2011). Its natural recharge is ensured by meteoric water and the Wadi runoffs (Ennabli, 1980; Rekaya, 1987). The deep aquifer is a more explicitly multi-layered system composed of ancient Quaternary deposits located in the central part of the plain, the Miocene and Oligocene sandstone series as well as the Eocene limestone formations that outcrop along the plain boundaries. Productive series are located usually at depths reaching more than 100 m (Farhat, 2011; Hechemi, 1989). In the focus area of the El Hma watershed, shallow and deep aquifers of Mio-

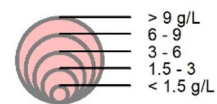
Plio-Quaternary units are exploited mostly by dig and tube wells at depths ranging from 15 to 120 m. The transmissivity of these heterogeneous deposits ranges between 0.1×10^{-3} and $8 \times 10^{-3} \text{ m}^2/\text{s}$, and their storage coefficient varies between 6×10^{-3} and 7.3×10^{-5} (Rekaya, 1987; Jarraya-Horriche, 2004). The unconfined groundwater contour map of the focus area shows a shallow flow mostly influenced by topography (Fig. 3). In fact, three main flow axes can be distinguished: (i) a SW → NE flow from the recharge zone at the Majoura mount

Legend

- △ Wadi sample
- ▲ Dam water sample
- Shallow well sample
- Deep well sample

- Check dam
- - - - - Sewer pipe

TDS (g/L)



- Cement factory site
- El Hma dam
- Groundwater contour (m)
- ➔ GW flow direction

Hydrological network

- River
- Principal
- - - - - Intermittent

Elevation

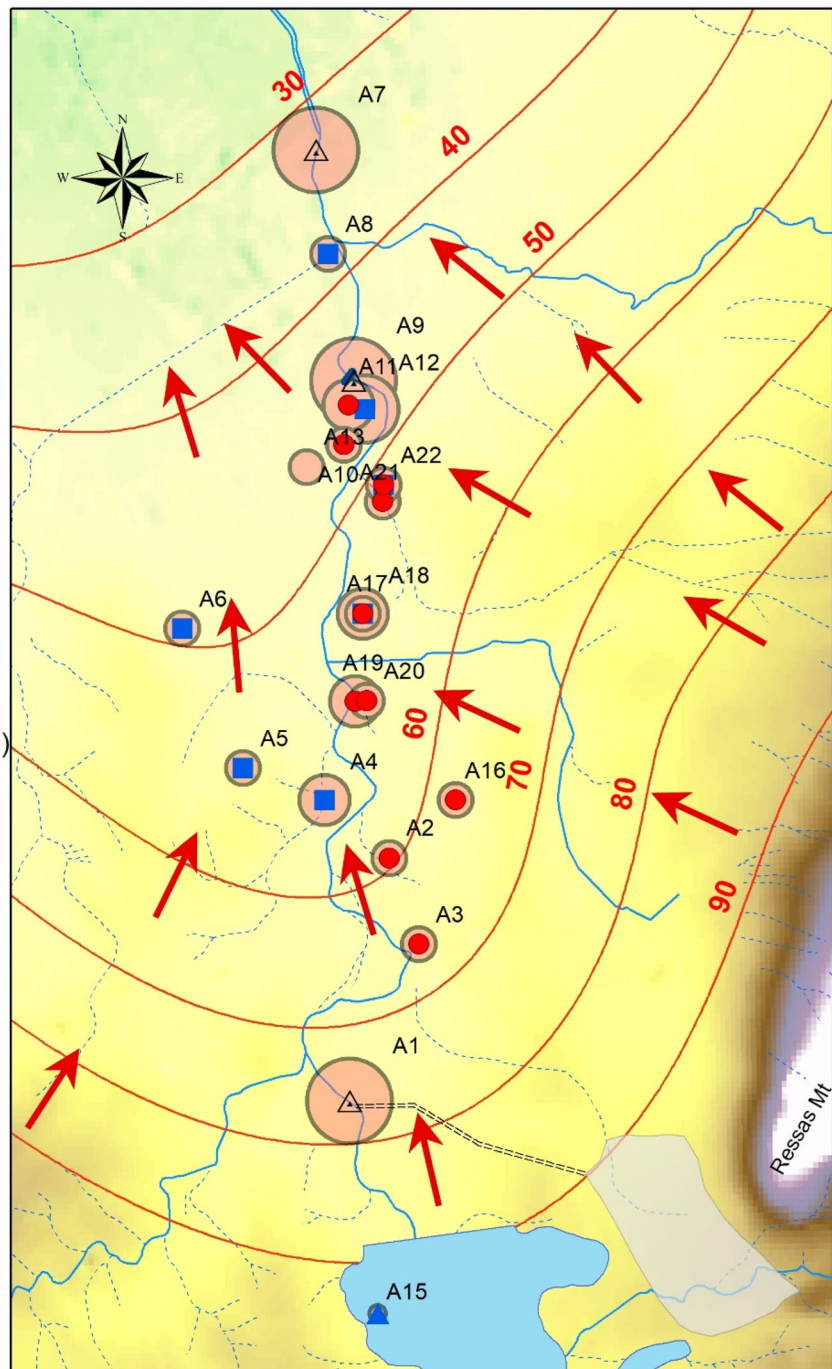
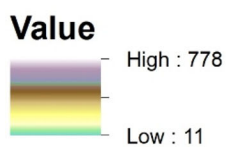


Figure 3. Spatial distribution of water samples' total dissolved solids superposed with groundwater contour lines.

pedmont toward the central part of the plain; (ii) a S → N groundwater flow from the hill dam on the way to the plain center describing a possible underflow beneath the Wadi; and (iii) a SE → NW

groundwater flow from the recharge zone at the pedmont of Ressas Mountain to the plain center. The Wadis contribute to the aquifer recharge, especially in the immediate upstream of the check

dam, which was built originally to enhance the Wadi water infiltration during humid periods or artificial hill dam water releases.

MATERIALS AND METHODS

Water Sampling and Analysis

In total, 22 water samples were collected from surface water bodies (dam and Wadi) and groundwater (shallow and deep aquifers) during a field survey in June 2019. The sampling strategy consisted of taking all the existing wells in the vicinity of the Wadi. We considered a buffer zone not exceeding 500 m from the Wadi, wherein we collected the water samples. According to Ben Farhat (2011) (2011, Charef et al. (2012) and Ben Moussa et al. (2020), there are no significant seasonal variations in groundwater quality between wet and dry seasons. Therefore, a single sampling survey was considered to furnish reliable information regarding the AAR occurrence in the El Hma plain.

The water samples were taken after the stabilization of electrical conductivity (EC), and they were collected in clean high-density polyethylene (HDPE) bottles. Temperature, pH, EC and groundwater level were measured in situ. In the laboratory, bicarbonate (HCO_3^-) was analyzed using the titration method with sulfuric acid. Major chemicals ions (anions Cl^- , SO_4^{2-} , NO_3^- and cations Na^+ , Ca^{2+} , Mg^{2+} , K^+) were analyzed by ion liquid chromatography (IC 732) and atomic absorption spectrometry (PerkinElmer AAnalyst 200) at the Laboratory of Georesources, Water Research and Technologies Center (Borj Cedria Technopark, Tunisia). Stable isotopes (^{18}O and ^2H) were analyzed using an IsoPrime, GV Instruments, mass spectrometer at the HydroSciences LAMA laboratory (Montpellier, France) with 0.06 and 0.8‰ error measurement, respectively, for oxygen-18 and deuterium. Stable isotopes contents were quantified in the usual δ notation, thus:

$$\delta^2H() = \left[\frac{\left(\frac{^2H}{^1H}\right)_{\text{sample}}}{\left(\frac{^2H}{^1H}\right)_{\text{standard}}} - 1 \right] \times 10^3 \quad (1)$$

$$\delta^{18}O() = \left[\frac{\left(\frac{^{18}O}{^{16}O}\right)_{\text{sample}}}{\left(\frac{^{18}O}{^{16}O}\right)_{\text{standard}}} - 1 \right] \times 10^3 \quad (2)$$

As shallow groundwater is mainly used for irrigation in the Wadi El Hma plain, a set of quality assessment indices were calculated (Table 1).

Electrical Resistivity Tomography (ERT) Survey

ERT is a geophysical method based on the resistivity contrast. It is used to determine the resistivity of earth materials and their distribution in the subsurface. This approach is particularly applied in the case of large resistivity contrast to delineate the interface between saline and freshwater (Bauer et al., 2006; Chabaane et al., 2017; McInnis et al., 2013).

ERT measurements were performed in the same period as the piezometric and geochemical survey (June 2019) using an ABEM SAS-4000 resistivity meter. Wenner array configuration was used to delineate accurately the interface between freshwater and brackish/saline water (Baharuddin et al., 2013; Loke, 2011). It also provides a good sensitivity for vertical heterogeneities, allowing better differentiation of plumes' structures (Doetsch et al., 2012; Kemna et al., 2002). ERT profiles were performed using 64 stainless steel electrodes set 5 m apart. The obtained resistivity data were inverted using RES2DINV software based on the smoothness-constrained least-square method (Loke & Barker, 1996; Loke & Dahlin, 2002).

RESULTS AND DISCUSSION

Hydrochemical Data

Geochemical tracers including major chemicals and stable isotopes are essential tools for understanding the hydrogeochemical functioning of aquifers. Hydrochemical and isotopic characteristics of the waters sampled from the Wadi El Hma plain are summarized in Table 2. Water temperature and pH varied from 17 to 27 °C and 7.5 to 9.9, respectively. The EC of the groundwater sample ranged from 2.1 to 8.2 mS/cm, and that of surface water varied between 0.6 (dam) and 27 mS/cm (Wadi water). The high EC values of Wadi water may be due to saline water discharge from a neighboring cement factory, which rejects its wastewater effluent directly into the dry Wadi channel through a sewer pipe. The spatial distribution of water salinity revealed that wells located in the proximity of the Wadi and within the

Table 1. Indices of groundwater suitability for irrigation: sodium adsorption ratio (SAR), percentage of sodium (%Na), permeability index (PI) and electrical conductivity (EC)

Index	Equation	Range	Water class	Reference
SAR	$\frac{Na^+}{\sqrt{\frac{Ca^{2+}+Mg^{2+}}{2}}}$	< 10	Good	Richards (1954)
		10 – 18	Permissible	
		18 – 26	Doubtful	
		> 26	Unsuitable	
%Na	$\frac{Na^++K^+}{Ca^{2+}+Mg^{2+}+Na^++K^+} \times 100$	< 40	Good	Wilcox (1948, 1955)
		40 – 60	Permissible	
		60 – 80	Doubtful	
		> 80	Unsuitable	
PI	$\frac{Na^++\sqrt{HCO_3^-}}{Ca^{2+}+Mg^{2+}+Na^+} \times 100$	< 25	Good	Doneen (1964), Eaton (1950)
		25 – 50	Permissible	
		50 – 75	Doubtful	
		> 75	Unsuitable	
EC	Electrical conductivity ($\mu\text{S/cm}$)	< 750	Good	Follet and Soltanpour (1985), Bauder al (2011)
		750 – 1500	Permissible	
		1500 – 3000	Doubtful	
		> 3000	Unsuitable	

Table 2. Physicochemical, major elements and stable isotopes data from water samples collected from the Wadi El Hma plain

Category	Range	Field measurement			Laboratory analysis (major elements, in mg/l)								Stable isotopes (in ‰ vs SMOW)	
		T (°C)	pH	EC (mS/ cm)	HCO ₃ ⁻	Cl ⁻	NO ₃ ⁻	SO ₄ ²⁻	Na ⁺	K ⁺	Mg ²⁺	Ca ²⁺	¹⁸ O	² H
Surface wa- ter	Min	20.1	8.5	0.7	148.3	61.3	0.0	109.7	53.8	1.9	17.3	63.1	-5.7	-32.9
	Max	27.0	9.9	27.2	1321.3	8302.5	1.6	2297.9	6937.2	106.7	242.9	1002.8	-1.1	-9.5
	STD	2.8	0.6	10.1	432.8	3395.0	0.7	918.0	2692.7	41.0	87.8	366.8	2.0	10.0
Shallow GW	Min	17.0	7.6	2.1	482.6	253.3	31.3	413.9	224.0	3.9	68.6	274.9	-5.1	-30.0
	Max	22.1	8.0	5.6	683.3	1252.3	79.9	766.3	1067.0	10.2	120.6	389.2	-1.7	-11.8
	STD	1.6	0.1	1.1	77.5	334.5	17.3	124.5	288.1	2.0	20.0	45.5	1.3	7.6
Deep GW	Min	19.7	7.5	2.1	477.3	377.2	8.2	225.3	278.5	5.0	56.2	210.7	-5.6	-32.8
	Max	23.3	7.9	8.2	886.3	2243.5	43.1	795.9	1489.5	12.3	143.1	626.0	-2.6	-16.5
	STD	1.4	0.1	2.2	155.3	724.4	13.4	220.2	478.5	2.8	33.5	144.7	1.4	7.7

STD standard deviation

groundwater flow pathways particularly show high values of total dissolved solids (TDS) exceeding 6 g/l (Fig. 3). This suggests the occurrence of an AAR process consisting of infiltration of saline Wadi water and its migration within the saturated zone. For all the water samples collected during the survey, Na⁺ was the dominant cation and the order of mean concentration of cations was Na⁺ > Ca²⁺ > Mg²⁺ > K⁺, while Cl⁻ was the dominant anion and the order of mean concentration of anions was Cl⁻ > HCO₃⁻ > SO₄²⁻ > NO₃⁻.

Classification of Water Samples

Classification of water samples into groups facilitates segregation of relevant analytical data to understand the sources of dissolved constituents. Alternatively, it can serve to comprehend the mineralization processes that occur during AAR. Presenting the hydrochemical data in charts and graphs like the Piper diagram helps in classifying water samples according to their geochemical facies (Piper, 1944). It is among the simplest and widely used diagrams to assess groundwater quality in many regions in Tunisia (e.g., Chekirbane et al., 2013; La-

chaal et al., 2014; Mlayah et al., 2011). The Piper diagram of the water samples from the study area shows that Wadi water and brackish groundwater samples located in the vicinity of the Wadi are characterized by Na–Cl facies, whereas the remaining dam water and fresh groundwater samples were of the Ca–SO₄–Cl type (Fig. 4). Focusing on the ternary diagram of anions, a tendency toward the Cl pole was observed, suggesting the existence of a mixing phenomenon as a principal conductor of water salinization. A tendency of migration toward the Na pole is observed in the cation ternary diagram, which may indicate the occurrence of cation exchange during the salinization process. In a regional flow scale, a slightly similar behavior was reported by previous studies that focused on the whole aquifer of the Mornag plain (Farhat et al., 2010; Moussa et al., 2020).

Salinization Process

The bivariate diagram of sodium versus chloride shows two main groups (Fig. 5). The first group of samples indicates a flawless correlation between Na and Cl, in which the fresh shallow water and deep groundwater samples (particularly the Ca–SO₄–Cl type) fall on the 1:1 line. This suggests halite dissolution as the origin of these two elements. The second group of samples comprises the saline Wadi water and brackish groundwater samples (Na–Cl type); they deviate from the halite dissolution line. Thus, besides the geological effect, another phenomenon such as salt intrusion likely governs the salinization of water in the area. The evolution from fresh groundwater (i.e., Ca–SO₄–Cl type) to a salty groundwater enriched by Na⁺ and Cl[−] is proof of mixing with a saline water body, which may be the formerly infiltrated saline Wadi water in the vicinity of the check dam.

The cation exchange between sodium and calcium or magnesium ions may explain the excess of Na⁺ concentration (Stimson et al., 2001). In addition to the dominance of Na⁺ and Cl[−] in groundwater samples belonging to the group “Shallow well (3),” these samples show relative enrichment in bicarbonate. The excess in HCO₃[−] may cause the release of Na⁺ into the solution by exchange reaction with the exchange sites (Jalali, 2007). In order to confirm the cation exchange phenomena as a conducting process for groundwater salinization in the Wadi El Hma plain, the plot of Na⁺ + K⁺ – Cl[−] versus Ca²⁺

+ Mg²⁺ – SO₄^{2−} – HCO₃[−] was examined (Fig. 6). The difference between the sum of sodium and potassium from one side and the chloride from the other side represents the amount of Na⁺ and K⁺ gained or lost relative to that provided by the geological effect (halite dissolution). In contrast, the difference between the sum of calcium and magnesium from one side and the sum of sulfate and bicarbonate from the other side points out any gained or lost Ca²⁺ and Mg²⁺ relative to that provided by gypsum, calcite and dolomite dissolution. In the absence of any exchange with saline bodies, all data should be plotted close to the origin (McLean et al., 2000). However, in the occurrence of the cation exchange phenomenon, the relation between these two parameters should be linear and significantly negatively correlated. Among the plotted samples in Figure 6, the brackish and saline groundwater samples show negative correlation of the two parameters: The increase in Na⁺ + K⁺ may be related to a decrease in Ca²⁺ + Mg²⁺ or an increase in HCO₃[−] + SO₄^{2−}. Therefore, the main process controlling the salinization of groundwater in the Wadi El Hma plain would be cation exchange. This phenomenon suggests the presence of a saline water body that consists of the infiltrated saline Wadi water. The cation exchange responsible such kind of salt intrusion may be described as:



In aquifers holding clayey materials, natural softening or ion exchange may take place (Hounslow, 2018). As shown in Eq. 3, calcium is absorbed by the exchanger X whereas sodium is released to subsequently form Na–Cl type water.

Tracing of AAR with Stable Isotopes

The stable isotopes composition of the water samples from the Wadi El Hma plain is plotted in Figure 7. Isotope contents range from − 5.7 to 1.1‰ V-SMOW and between − 32.9 and − 9.5‰ V-SMOW for δ¹⁸O and δ²H, respectively. For the samples depleted with a d-excess showing no or low evaporation process (> 7.5), a distinction can be made between the deep groundwater (more depleted − 5.25‰ and − 31.2‰, respectively, for oxygen-18 and deuterium (5 points)) and the shallow aquifer (− 4.49‰ and − 27.4‰, respectively, in oxygen-18 and deuterium (4 points)). Compared

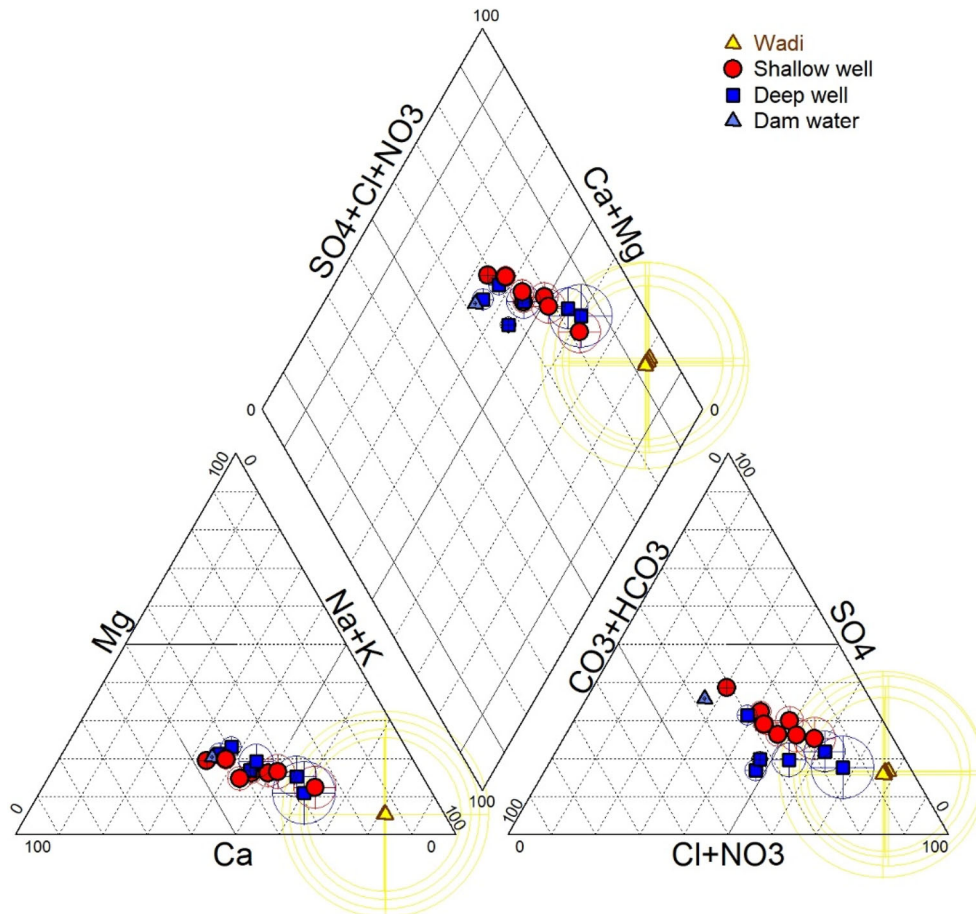


Figure 4. Piper diagram for water samples.

with the mean isotope content of rainfall at Tunis station over the 1967–2006 period (<https://www.iaea.org/resources/network/global-network-of-isotopes-in-precipitation-gnip>), the little more depleted value in deep aquifer (-4.38‰ and -25.4‰) could be due to the recharge zone with altitudes higher those that constitute the hills delimiting the catchment (400–700 a.m.s.l.). This formation corresponds to the deep groundwater whereas the recharge zone of shallow aquifer has altitudes lower than 200 a.m.s.l. The water flowing in the Wadi in June represents only the sewage from the cement factory and it shows isotope content close to the isotope value of the deep groundwater. In fact, the water used in production and cleaning processes in the cement factory is pumped into the deep groundwater and then rejected into the sewer system to reach the Wadi El Hma.

Based on the delta diagram, two clusters can be distinguished. The first group, which clearly deviates from the GMWL: $\delta^2\text{H} = 8 \delta^{18}\text{O} + 10$ (Craig, 1961; Rozanski et al., 1993) and the LMWL of Tunis–Carthage GNIP: $\delta^2\text{H} = 8 \delta^{18}\text{O} + 12.4$ (Zouari et al., 1985), is composed of enriched isotopes composition of the dam water and mainly phreatic groundwater samples located in the upstream region of the plain near the El Hma hill dam. These samples are also affected by evaporation, which is marked with a low d-excess (1.7–5.2) and follows a trend line with the equation: $\delta^2\text{H} = 4.17 \delta^{18}\text{O} - 5.22$ ($R^2 = 0.94$). This suggests a possible role of aquifer recharge from the hill dam water body in the upstream zone, which presents moderate EC (2.1–2.8 mS/cm). In contrast to the middle zone near the check dam, evaporated shallow water has higher EC (3.5–5.5 mS/cm) highlighting another complementary process, which could be infiltration from the Wadi or water irriga-

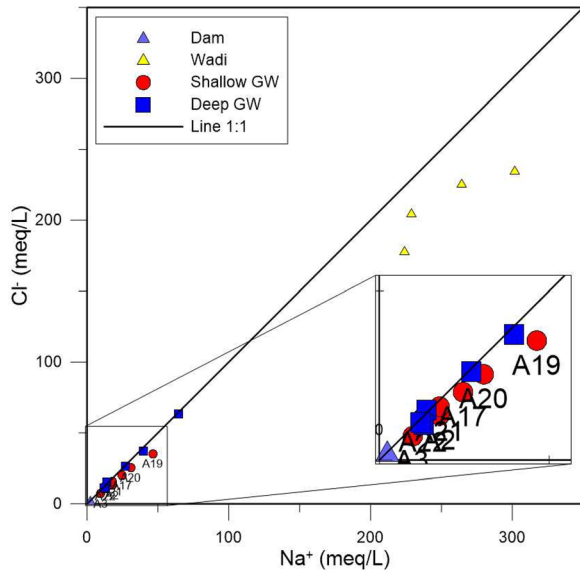


Figure 5. Plot of Na^+ versus Cl^- .

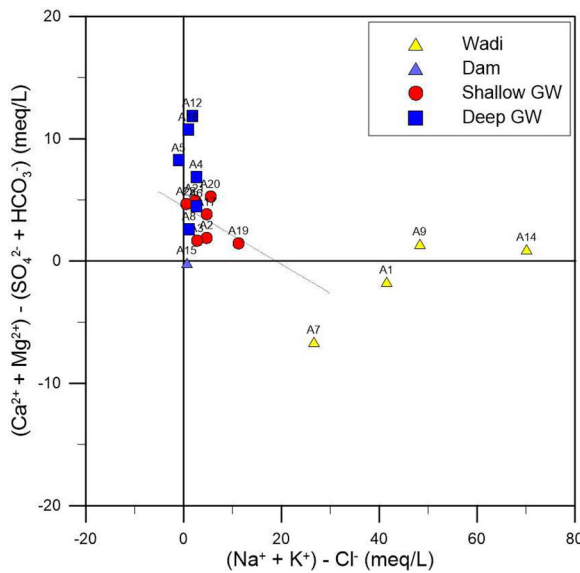


Figure 6. Plot of $\text{Na}^+ + \text{K}^+ - \text{Cl}^-$ versus $\text{Ca}^{2+} + \text{Mg}^{2+} - \text{SO}_4^{2-} - \text{HCO}_3^-$.

tion. With $\text{EC} = 2.6 \text{ mS/cm}$, deep groundwater samples located in the upstream zone far away from the Wadi (A5 and A6) are not affected by evaporation. In this zone, the deep aquifer seems totally isolated from the shallow aquifer. The two evaporated samples from a deep aquifer close to the Wadi (A4 upstream and A18 middle zone) show higher mineralization (4.8–5.3 mS/cm). In this case, hy-

draulic connection with shallow groundwater and the Wadi has to be considered. The second group with depleted stable isotopes content includes some points in deep groundwater isolated from the surface and with moderate EC, except one (A12) with the highest EC value (8.2 $\mu\text{S/cm}$), saline Wadi water and brackish shallow aquifer samples located near the check dam in the middle part of the plain. They almost fall on the GMWL and LMWL, confirming a rapidly infiltrated meteoric water origin. Paradoxically, these samples (except isolated points in deep aquifer) are characterized by high salt content. As previously mentioned, the Wadi water is simply discharged saline water coming from the cement factory, pumped from a deep well, used in production and cleaning processes and then rejected into the sewer system to reach Wadi El Hma. The similar stable isotopes content of this effluent compared to the wells located in the vicinity of the check dam suggests the role of this effluent in AAR and groundwater salinization in this zone.

The biplot of $\delta^{18}\text{O}$ versus Cl^- is an effective tool for differentiating salinity origins. It has been applied in several AAR cases (e.g., Chekirbane et al., 2013; Kammoun et al., 2018; Mejri et al., 2018). The water samples affected by saltwater coming from the cement factory were characterized by an increase in chloride content versus depleted stable isotope content. However, the water samples affected by evaporation had an opposite behavior marked by enrichment in stable isotopes content associated with reduced chloride concentration linked to low mineralization of surface water (Clark & Fritz, 1997). Plotted in Figure 8, the water samples from the Wadi El Hma plain are clustered in two main groups: (i) dam water and fresh groundwater located in the upstream of the plain near the hill dam, which are mainly affected by evaporation; and (ii) saline Wadi water and brackish groundwater located near the check dam, where salt intrusion as salinization process is confirmed. Some points could be the result of mixing of the two processes or may be the result of infiltration of irrigated water; in contrast, other points from deep groundwater showed no evidence of anthropogenic influence.

Monitoring of Brackish/Saline Groundwater Plume Using Geoelectrical Data

Geoelectrical methods such as ERT are effective tools that provide accurate images of saline and

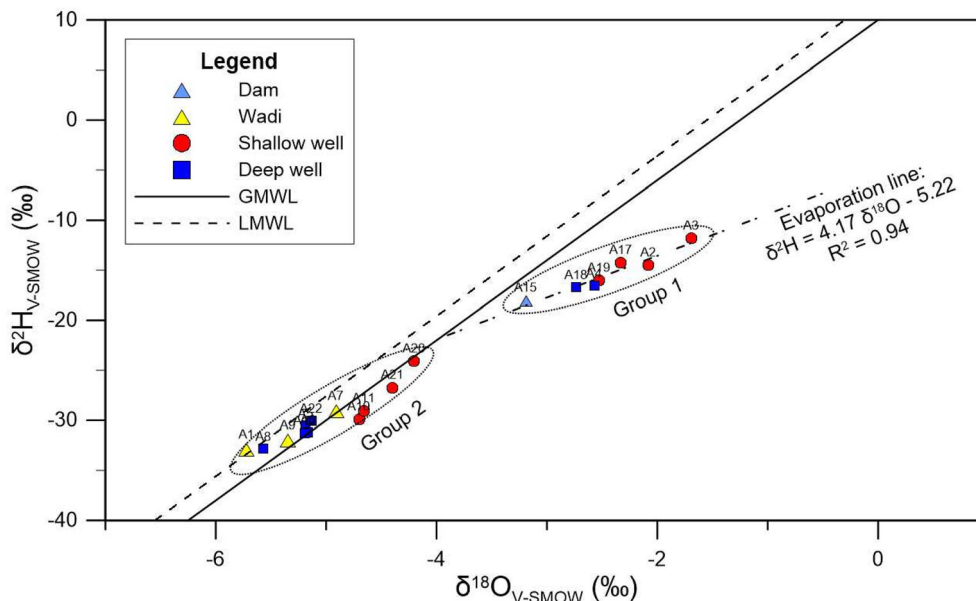


Figure 7. Delta diagram ($\delta^{18}\text{O}$ vs $\delta^2\text{H}$) of the water samples from the Wadi El Hma plain.

brackish water plumes in subsurface environments (e.g., Singha & Gorelick, 2005; Chabaane et al., 2018; Doetsch et al., 2012). Two ERT profiles were carried out in the most salinized part of the aquifer, in the immediate vicinity of the Wadi El Hma and just upstream of the check dam (Fig. 9). The multi-electrode ABEM SAS-4000 Terrameter was used with a set of 32 electrodes and a regular electrode spacing of 10 m. The Wenner α configuration was used because of its excellent signal-to-noise ratio (Naudet et al., 2004). The first profile (P1) with a total length of 310 m was laid along the main groundwater flow direction from the Wadi toward the left side of the plain in order to delineate the saline/brackish water plume in the affected area. The second profile (P2) was longitudinally set to the Wadi meander close to its left bank along a distance of 315 m from the check dam for the purpose of detecting the contribution of the saline Wadi water in aquifer salinization.

Profile P1 showed relatively high resistivity values (40–60 $\Omega\cdot\text{m}$) near the Wadi left bank, which are due to the relatively dry silty sand (unsaturated vadose zone). Low resistivity values (< 10 $\Omega\cdot\text{m}$) appeared at 50 m far from the Wadi within depths of more than 30 m. These represent the interface between fresh and saline groundwater (Fig. 10). The deep well A12 pumps water within this plume, explaining its high EC (8.2 mS/cm). The shape of the

brackish/saline water plume is not regular due to the abundant heterogeneous Quaternary deposits. In fact, located at a distance of less than 100 m from A12, the shallow well (25 m depth) A11 shows a lower EC value (5.2 mS/cm) because the saline plume emanates from deeper horizon. The low resistivity values found at 5 m depth near A11 well represent soils irrigated with the brackish water (Fig. 10).

Profile P2 show low values of resistivity (< 10 $\Omega\cdot\text{m}$) near the check dam at depths of less than 5 m. These data represent the inlet of saline water toward the saturated zone. Almost all the subsurface environment in depths more than 5 m below the Wadi bed are favorable ways of the AAR of the aquifer.

Mapping and Assessment of Water Suitability for Irrigation

Water resources in the Wadi El Hma watershed are used mainly for irrigation. Therefore, an assessment of the suitability of these waters for irrigation is essential in order to preserve soil and increase crop yield in the region. Certain indices are used to assess water stress using physical and hydrodynamic parameters of aquifers (Nayyeri et al., 2021). However, in the present case, the suitability assessment was performed using the following in-

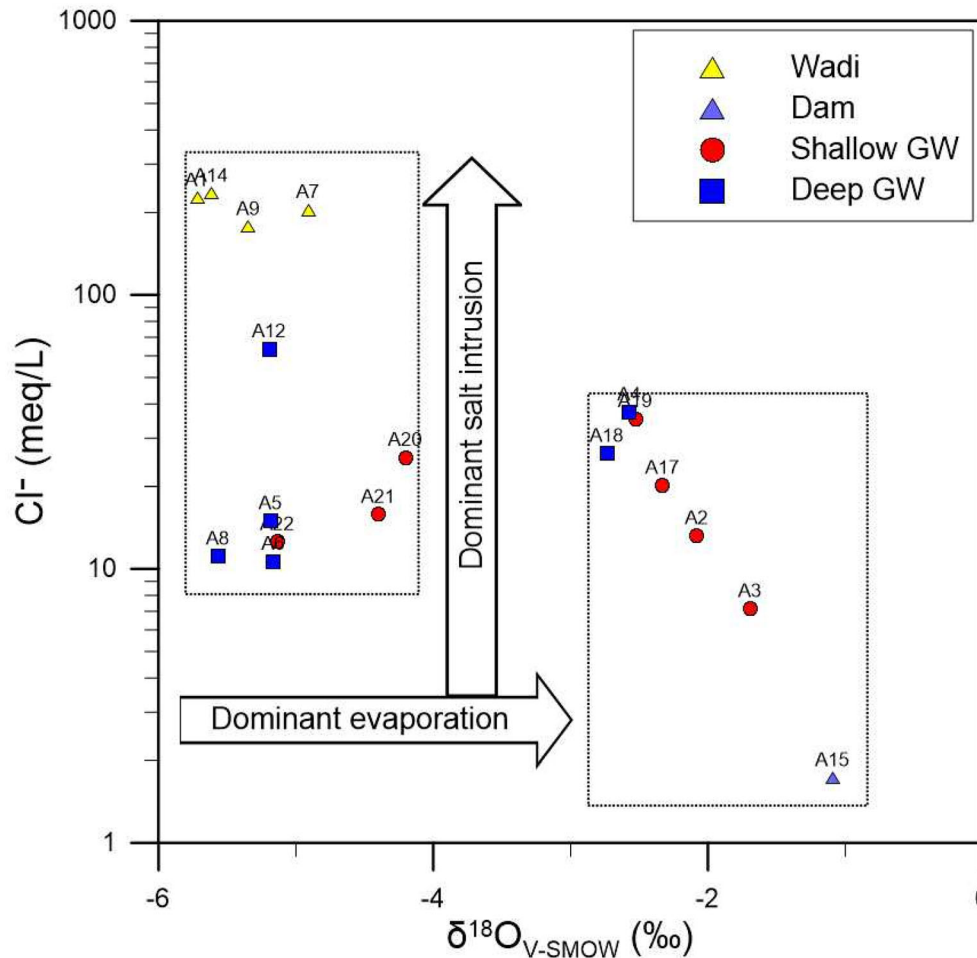


Figure 8. Diagram of salinization origin ($\delta^{18}\text{O}$ vs Cl^-).

dices based on hydrochemical characteristics of the available water: sodium adsorption ratio (SAR), percentage of sodium hazard (%Na) and permeability index (PI).

SAR is a ratio of sodium ions to the sum of calcium and magnesium ions present in a water sample. It is used to estimate the potential of sodium ions to accumulate in the soil primarily at the expense of the other major cations as a result of regular use of sodic water (Bouwer & Idelovitch, 1987). Water suitability for irrigation using SAR was classified by Richards (1954) (Table 1). Percentage of sodium hazard (%Na) is an index proposed by Wilcox (1948) to categorize any source of water for irrigation use. Sodium cation is known to make chemical bonding with soil to reduce unsaturated water movement (Ayers and Westcot, 1985). Crop

growth and yield are particularly reduced in sodium-affected soil (Todd and Mays, 2004). The use of sodium-enriched water in irrigation leads to ions tending toward clay particles by removing calcium and magnesium cations through a base-exchange reaction that reduces water movement capacity within the irrigated soils (Rengasamy & Olsson, 1993; Rhoades et al., 1968). The PI is used to assess water movement aptitude in long-term irrigated soils based on their contents in bicarbonate, sodium, calcium and magnesium ions (Doneen, 1964). Besides, water EC should obviously be taken into consideration because it represents TDS. Salt excess can increase the osmotic pressure of soil solution especially under drought conditions leading to major difficulties for plant uptake and growth (Bauder et al., 2011; Zaman et al., 2018).

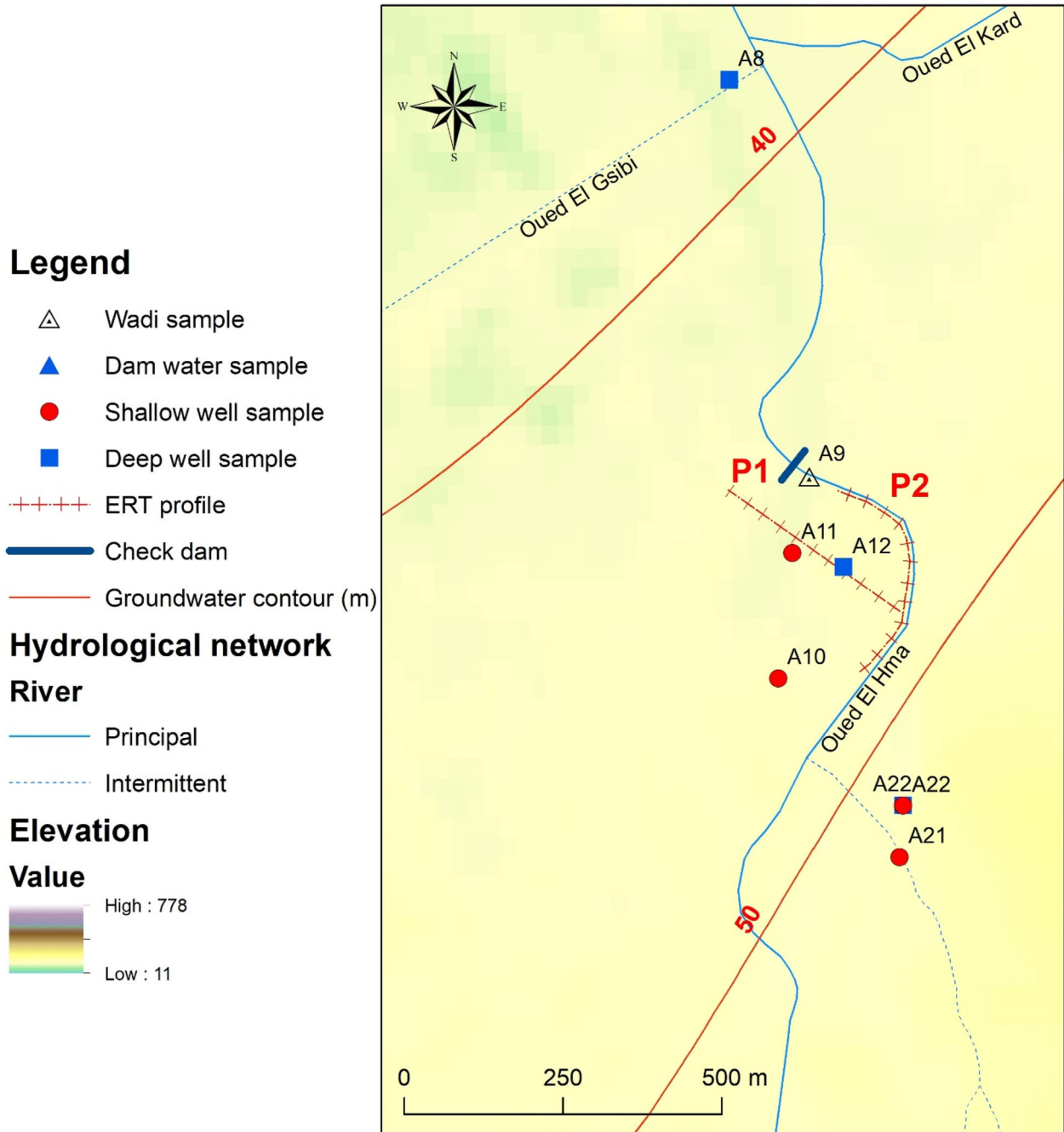


Figure 9. Location of the ERT profiles.

The four parameters chosen to assess suitability for irrigation do not have the same importance. Therefore, a multi-criteria decision approach, namely analytic hierarchy process (AHP) developed by Saaty (2000), was applied to determine the weight

of each parameter. AHP is used widely in assessing water potential in complex aquifers (e.g., Zaree et al, 2019). In the present case, a pairwise comparison matrix was established (Table 3). A 1–9 point scale was adopted to assess the relative

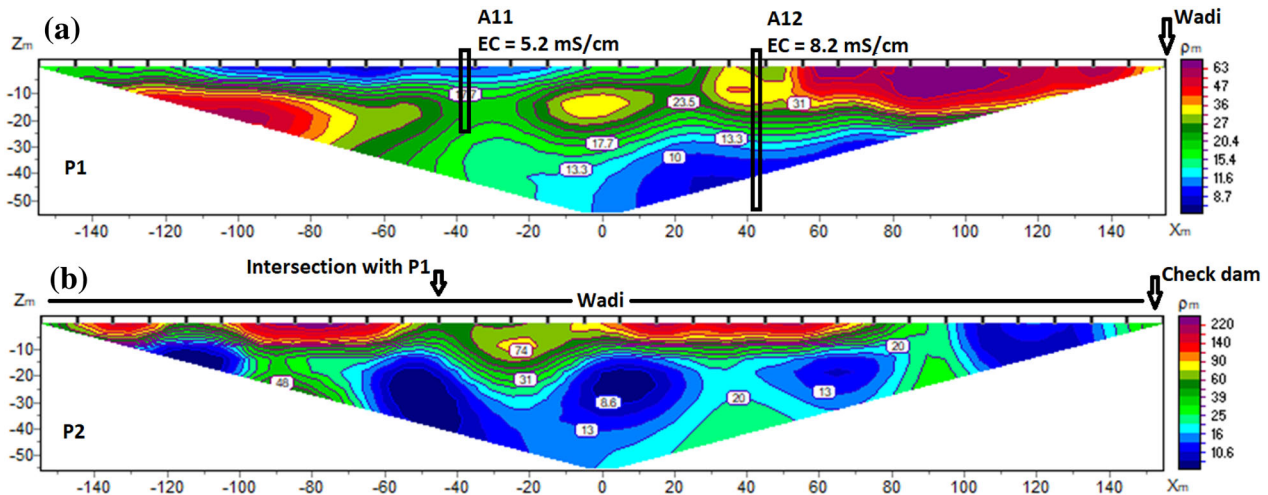


Figure 10. Inverted resistivity profiles: (a) Profile P1; (b) Profile P2.

Table 3. Pairwise comparison matrix and weights of parameters based on AHP

	SAR	%Na	PI	EC	Weight
SAR	1	2	1	2	34.6%
%Na	1/2	1	1	1/2	16.3%
PI	1	1	1	1/2	20.5%
EC	1/2	2	2	1	28.6%

importance in terms of suitability for irrigation among the chosen parameters. The weight values of the parameters are given in Table 3; they reflect the relative importance of each criterion. The relative weights are calculated using the eigenvector corresponding to the largest eigenvalue (Mishra et al., 2015). In addition, the consistency of the pairwise comparison matrix should be controlled by means of a control value called the consistency ratio (CR). The CR expresses the random probability of values obtained in a pairwise comparison matrix (Malczewski, 1999). If the value of CR is less or equal to 10%, the pairwise comparison decisions are sufficiently consistent (Saaty, 2005). The CR for the present matrix is 7%; thus, the obtained weights can be considered.

Once the SAR, %Na and PI have been calculated and reclassified using scores in a 1–4 scale (1 = good; 2 = permissible; 3 = doubtful; 4 = unsuitable), an irrigation suitability index (ISI) was calculated as:

$$ISI = \sum_{i=1}^3 s_i w_i \quad (4)$$

where s_i and w_i represent the score and weight, respectively, of parameter i . Then, a map of spatial distribution of ISI was created using ArcGIS software (Fig. 11). This map shows clearly that all the Wadi water samples were unsuitable for irrigation. However, the dam water, deep groundwater and shallow groundwater samples located in the upstream region of the plain were mostly good to permissible for irrigation. Samples located in the vicinity of the check dam were classified doubtful regarding their suitability for irrigation.

Integrated Conceptual Modeling and Its Implications

Following the above-discussed integrated approach involving all the analytical techniques used in the present study, a conceptual model for the understanding of the hydrogeochemical functioning of the aquifer as well as for detailing the processes of groundwater recharge was developed (Fig. 12). The El Hma plain is characterized by a shallow groundwater flow type that is controlled mainly by topography. The piedmont of the Ressas Mountain and the relatively high relief areas constitute the main natural recharge zones. Wadi El Hma, which is almost dry all the year, constitutes the downstream

Legend

- △ Wadi sample
- ▲ Dam water sample
- Shallow well sample
- Deep well sample

ISI

- Good
- Permissible
- Doubtful
- Unsuitable

- Check dam
- El Hma dam

Hydrological network

- River
- Principal
- Intermittent

Elevation

- Value**
- High : 778
 - Low : 11

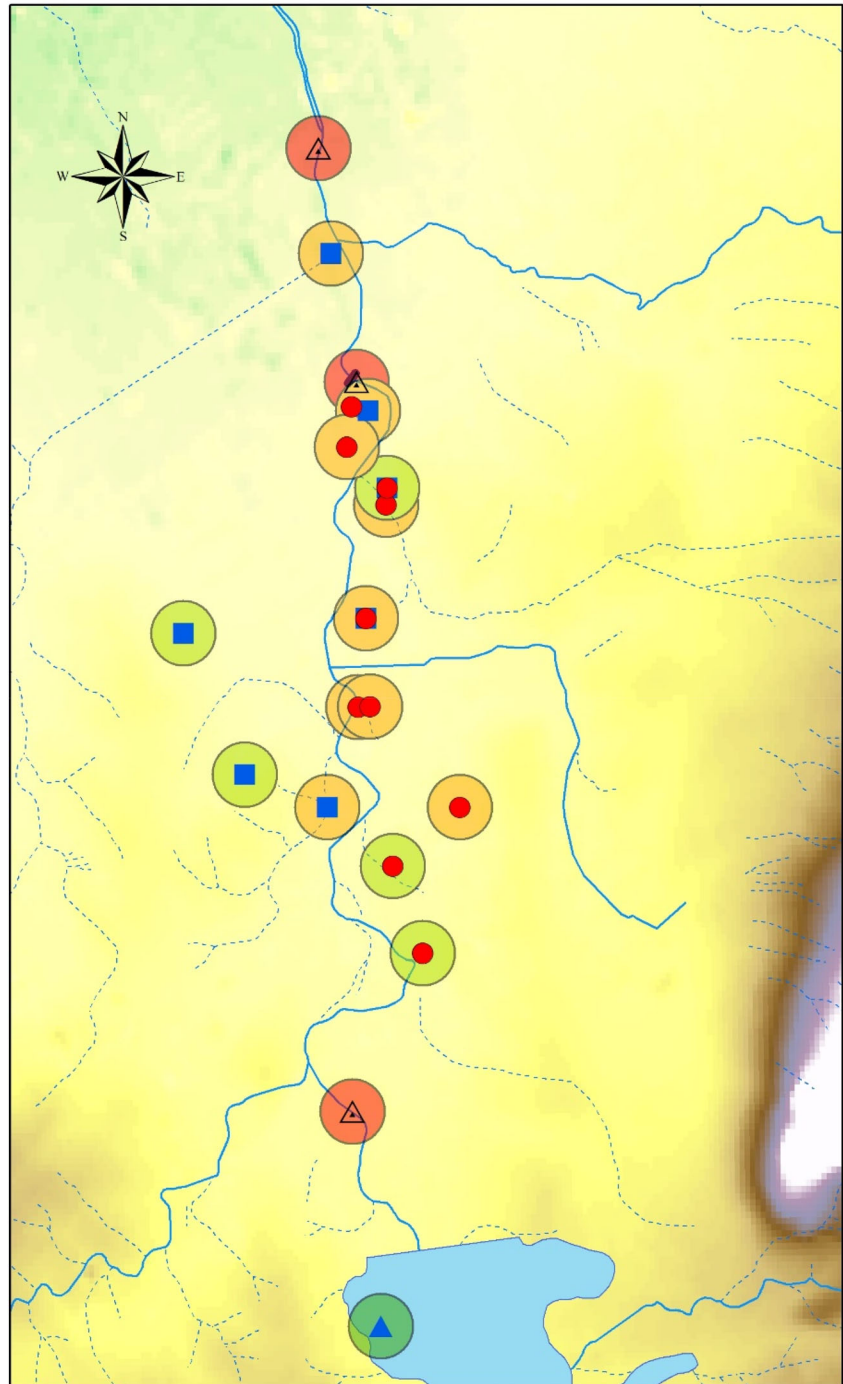


Figure 11. Spatial distribution of ISI in the Wadi El Hma plain.

channel where dam water is occasionally discharged to enhance aquifer recharge using a check dam. A discharged saline water with TDS of 27 mS/cm is

mixed with the Wadi water. This water mixture often constitutes the main runoff in the Wadi, and it easily reaches the constructed check dam where it

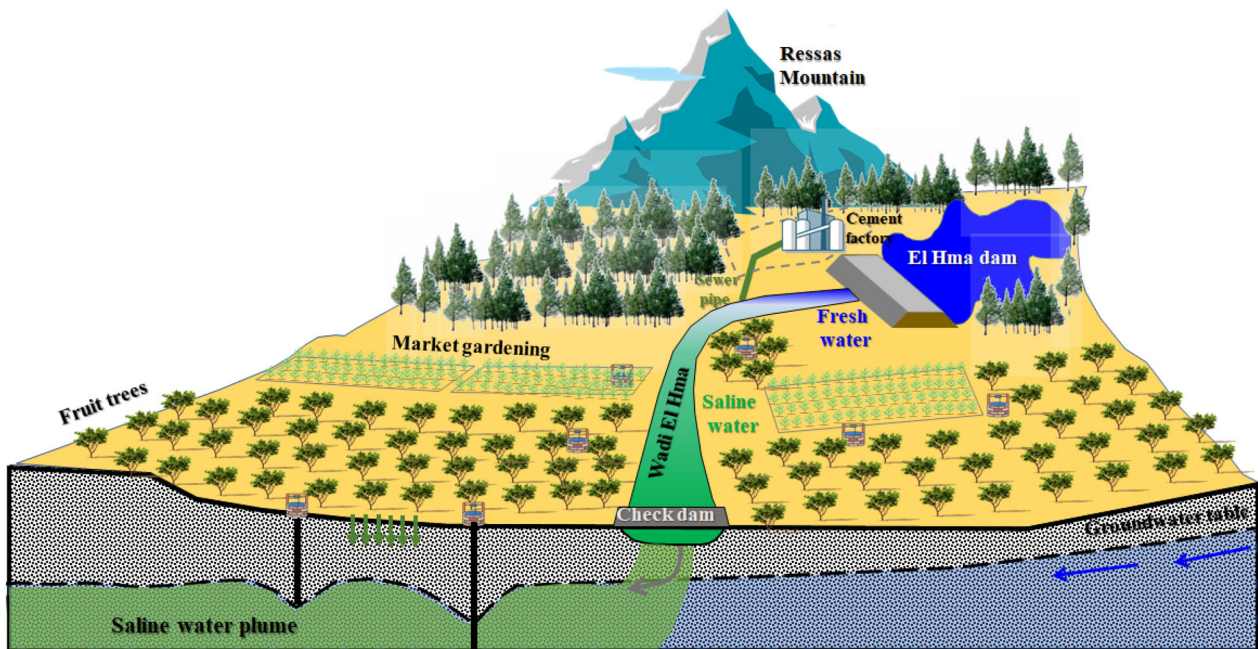


Figure 12. Integrated conceptual model of groundwater flow system at the Wadi El Hma plain.

infiltrates and migrates toward the shallow aquifer. The saline water plume was detected at a distance of 200 m far from the check dam and at depths around 30 m. The affected wells are pumping brackish water classified as doubtful for use in irrigation. However, it is used effectively to irrigate lands and, consequently, it can be considered as an anthropogenic recharge for the local shallow aquifer.

The integrated approach based on hydrodynamic, geochemical and geophysical techniques was extremely useful for understanding the aquifer functioning and the impact of anthropogenic recharge sources. In fact, we proved that, in a poorly monitored hydrological system (such as the case of the El Hma plain), the combination of multi-disciplines is essential to furnish a complete picture of the system and to make it easier for decision-makers to propose suitable countermeasures for water sustainability.

CONCLUSIONS

Flood plain aquifers are critical sources of water in arid and semiarid regions of the world. However, increased pressure on these aquifers including over-pumping and AAR threatens their sustainable use.

This study implemented a multidisciplinary approach based principally on a combination of geochemical tracers and geoelectrical method, and this approach was used to elucidate the AAR processes in a reduced-scale agricultural floodplain and to assess its impacts on groundwater contamination and suitability for irrigation. The obtained piezometric and geochemical data reveal an interaction between the Wadi and the aquifer, especially in the downstream part of the plain near the check dam. At these locations, the Wadi plays the role of a losing system where saline water is infiltrated throughout its permeable bed, particularly in the immediate meander located before the check dam. This area is the most affected by salt intrusion due to the presence of the existing managed aquifer recharge infrastructure (check dam). Electric resistivity tomography profiles were extremely useful for delineating and monitoring the salt water plume. Transversely and following the main groundwater flow direction, infiltrated saltwater reached more than 50 m depth and contributed to the contamination of the neighboring wells where TDS exceeded 6 g/l. Longitudinally, low resistivity values, which reveal the infiltrated saline Wadi water throughout the left bank, exist in the immediate proximity of the check dam, which represents the inlet toward the

saturated zone. The brackish/saline water plume generally starts from a depth of 5 m under the Wadi bed. This plume highlights the role of the Wadi and check dam in the AAR of the aquifer. The hydrochemical data proved that cation exchange was the main salinization process of groundwater in the affected area. Isotopic tracers confirmed the evidence of salinization in this area and gave additional information regarding the recharge process in the upstream region where the hill dam contributes to aquifer recharge through direct interaction with its surface water body. Groundwater sustainability in the plain is threatened because of the present status of AAR. In fact, most of the sampled wells were classified doubtful for irrigation and the water in these wells is a threat to soils and crops.

Overall, the obtained results of this study demonstrated the important influence that anthropogenic sources exert on groundwater sustainable use in the El Hma plain. These results should draw the attention of decision-makers and stimulate their reaction to stop any contamination effluent in the Wadi and enhance the artificial recharge by hill dam water release to tentatively flush the salt and dilute its effect on the aquifer.

REFERENCES

- Ali, B. H., M., Jedoui, Y., Dali, T., Ben Salem, H., & Memmi, L. (1985). Geological map of Tunisia at the scale 1/500 000, ed. Serv. Géol., Tunisia.
- Ayers, R. S., & Westcot, D. W. (1985). *Water quality for agriculture* (Vol. 29). Food and Agriculture Organization of the United Nations.
- Baharuddin, M. F. T., Taib, S., Hashim, R., Abidin, M. H. Z., & Rahman, N. I. (2013). Assessment of seawater intrusion to the agricultural sustainability at the coastal area of Carey Island, Selangor, Malaysia. *Arabian Journal of Geosciences*, 6(10), 3909–3928.
- Balleau, W. P. (2013). The policy of “pumping the recharge” is out of control. *Eos, Transactions American Geophysical Union*, 94(1), 4–4.
- Bauder, T. A., Waskom, R. M., Sutherland, P. L., & Davis, J. G. (2011). Irrigation water quality criteria. Fact sheet (Colorado State University. Extension). Crop series; no. 0.506.
- Bauer, P., Supper, R., Zimmermann, S., & Kinzelbach, W. (2006). Geoelectrical imaging of groundwater salinization in the Okavango Delta, Botswana. *Journal of Applied Geophysics*, 60(2), 126–141.
- Ben Farhat, B. (2011). Caractérisation de la géométrie des aquifères Mio-Plio-Quaternaires de la plaine de Mornag (NE Tunisie) par les méthodes géophysiques. Hydrochimie et modélisation de la recharge potentielle. Doctoral Thesis, Faculty of Sciences of Tunis, University of Tunis El Manar. 224p.
- Boutib, L. (1998). Tectonique de la région du grand Tunis: évolution géométrique et cinématique des blocs structuraux du Mésozoïque à l'Actuel (Atlas nord oriental de Tunisie). Doctoral dissertation, Faculty of Sciences of Tunis, University of Tunis El Manar, 151 p.
- Bouwer, H., & Idelovitch, E. (1987). Quality requirements for irrigation with sewage water. *Journal of Irrigation and Drainage Engineering*, 113(4), 516–535.
- Brown, D. G., Johnson, K. M., Loveland, T. R., & Theobald, D. M. (2005). Rural land-use trends in the conterminous United States, 1950–2000. *Ecological Applications*, 15(6), 1851–1863.
- Bujalka, P., Rakus, M., & Vacek, J. (1972). Geological map of Tunisia, La Goulette in 1/50 000 scale. Geological services of Tunisia, publ National Office of Mines, Tunisia.
- Chabaane, A., Redhaounia, B., & Gabtni, H. (2017). Combined application of vertical electrical sounding and 2D electrical resistivity imaging for geothermal groundwater characterization: Hammam Sayala hot spring case study (NW Tunisia). *Journal of African Earth Sciences*, 134, 292–298.
- Chabaane, A., Redhaounia, B., Gabtni, H., & Amiri, A. (2018). Contribution of geophysics to geometric characterization of freshwater–saltwater interface in the Maâmoura region (NE Tunisia). *Euro-Mediterranean Journal for Environmental Integration*, 3(1), 1–8. <https://doi.org/10.1007/s41207-018-0068-7>.
- Charef, A., Ayed, L., & Azzouzi, R. (2012). Impact of natural and human processes on the hydrochemical evolution of overexploited coastal groundwater: Case study of the Mornag aquifer refill (South-East Tunis, Tunisia). *Geochemistry*, 72(1), 61–69.
- Chekirbane, A., Tsujimura, M., Kawachi, A., Isoda, H., Tarhouni, J., & Benalaya, A. (2013). Hydrogeochemistry and groundwater salinization in an ephemeral coastal flood plain: Cap Bon Tunisia. *Hydrological Sciences Journal*, 58(5), 1097–1110.
- Clark, I. D., & Fritz, P. (1997). *Environmental isotopes in hydrogeology*. CRC Press.
- Closas, A., Imache, A., & Mekki, I. (2018). Groundwater governance in Tunisia. A Policy White Paper (No. 615–2018–4009).
- Craig, H. (1961). Isotopic variations in meteoric waters. *Science*, 133(3465), 1702–1703.
- Custodio, E. (2002). Aquifer overexploitation: What does it mean? *Hydrogeology Journal*, 10(2), 254–277.
- Doetsch, J., Linde, N., Vogt, T., Binley, A., & Green, A. G. (2012). Imaging and quantifying salt-tracer transport in a riparian groundwater system by means of 3D ERT monitoring. *Geophysics*, 77(5), B207–B218.
- Döll, P., & Flörke, M. (2005). Global scale estimation of diffuse groundwater recharge. Frankfurt Hydrology Paper 03. Institute of Physical Geography, Frankfurt University.
- Doneen, L. D. (1964). *Notes on water quality in agriculture*. University of California, Davis.
- Dregne, H. E. (1991). Global status of desertification. *Annals of Arid Zones*, 30(3), 179–185.
- Eaton, E. M. (1950). Significance of Carbonate in Irrigation Water. *Soil Science*, 69, 123–133.
- Ennabli, M. (1980). Etude hydrogéologique des aquifères du Nord-Est de la Tunisie pour une gestion intégrée des ressources en eau. Doctoral dissertation, University of Nice, France, 72p.
- Farhat, B. (2011). Caractérisation de la géométrie des aquifères Mio-plio-quaternaires de la plaine de Mornag (en Tunisie) par les méthodes géophysiques. Hydrochimie et modélisation de la recharge potentielle. Doctoral dissertation. University of Tunis El Manar, 208 p.
- Farhat, B., Mammou, A. B., Kouzana, L., Chenini, I., Podda, F., & De Giudici, G. (2010). Groundwater chemistry of the Mornag aquifer system in NE Tunisia. *Resource Geology*, 60(4), 377–388.

- Follett, R. H., & Soltanpour, P. N. (1985). Irrigation water quality criteria. Service in action; no. 0.506.
- Frija, A., Chebil, A., Speelman, S., & Faysse, N. (2014). A critical assessment of groundwater governance in Tunisia. *Water Policy*, 16(2), 358–373.
- Gleeson, T., Wada, Y., Bierkens, M. F., & Van Beek, L. P. (2012). Water balance of global aquifers revealed by groundwater footprint. *Nature*, 488(7410), 197–200.
- Godfray, H. C. J., Beddington, J. R., Crute, I. R., Haddad, L., Lawrence, D., Muir, J. F., Pretty, J., Robinson, S., Thomas, S. M., & Toulmin, C. (2010). Food security: The challenge of feeding 9 billion people. *Science*, 327(5967), 812–818.
- Healy, R. W., & Cook, P. G. (2002). Using groundwater levels to estimate recharge. *Hydrogeology Journal*, 10(1), 91–109.
- Hechemi, H. (1989). Explicative note of the water resources map of Tunisia at the scale 1/200 000 [Carte des ressources en eau de la Tunisie au 1/200 000. Notice explicative]. Technical Report, DGRE, Tunis, 19p.
- Hounslow, A. (2018). *Water quality data: Analysis and interpretation*. CRC Press.
- INM, 2018. Climatic data of Ben Arous prefecture. Institut National de la Météorologie, Tunis, Tunisia [online]. Available from: <http://www.meteo.tn/> [Accessed August 2018].
- Jalali, M. (2007). Salinization of groundwater in arid and semi-arid zones: An example from Tajarak, western Iran. *Environmental Geology*, 52(6), 1133–1149.
- Jarraya-Horriche, F. (2004). Contribution to the Analysis and the Rationalization of the Piezometric Network. Doctoral dissertation, University of Tunis El Manar Tunisia. 254p.
- Jarraya-Horriche, F. & Wolfgang, B. (2019). Seawater intrusion modelling in the Mornag aquifer, Tunisia. Proceedings of the 2nd ATLAS Georesources International Congress (AGIC219): Applied Geosciences for Groundwater. March 2019, Hammamet, Tunisia.
- Jauzein, A. (1967). Contribution à l'étude géologique de la Tunisie septentrionale: les confins de la dorsale tunisienne. *Ann. Mines et Géol.* 22, 475 p.
- Kammoun, S., Trabelsi, R., Re, V., Zouari, K., & Henchiri, J. (2018). Groundwater quality assessment in semi-arid regions using integrated approaches: The case of Grombalia aquifer (NE Tunisia). *Environmental Monitoring and Assessment*, 190(2), 87.
- Kemna, A., Vanderborgh, J., Kulesa, B., & Vereecken, H. (2002). Imaging and characterisation of subsurface solute transport using electrical resistivity tomography (ERT) and equivalent transport models. *Journal of Hydrology*, 267(3–4), 125–146.
- Lachaal, F., Chekirbane, A., Mlayah, A., Hjiri, B., & Tarhouni, J. (2014). A multi-tracer approach to understand the hydrogeochemical functioning of a coastal aquifer located in NE Tunisia. *IAHS Publication*, 363, 191–196.
- Leitão, T. E., Mota, R., Novo, M. E., & Lobo-Ferreira, J. P. (2014). Combined use of electrical resistivity tomography and hydrochemical data to assess anthropogenic impacts on water quality of a karstic region: A case study from Querença-Silves, South Portugal. *Environmental Processes*, 1(1), 43–57.
- Li, Z., Yang, Q., Yang, Y., Ma, H., Wang, H., Luo, J., Bian, J., & Martin, J. D. (2019). Isotopic and geochemical interpretation of groundwater under the influences of anthropogenic activities. *Journal of Hydrology*, 576, 685–697.
- Loke, M. H. (2011). Electrical resistivity surveys and data interpretation. In H. K. Gupta (Ed.), *Encyclopedia of solid earth geophysics* (2nd ed., pp. 276–283). Cham: Springer.
- Loke, M. H., & Barker, R. D. (1996). Practical techniques for 3D resistivity surveys and data inversion. *Geophysical Prospecting*, 44(3), 499–523.
- Loke, M. H., & Dahlin, T. (2002). A comparison of the Gauss-Newton and quasi-Newton methods in resistivity imaging inversion. *Journal of Applied Geophysics*, 49(3), 149–162.
- Malczewski, J. (1999). *GIS and multicriteria decision analysis*. Wiley.
- Maliva, R. G. (2020). Anthropogenic Aquifer Recharge. WSP Methods in Water Resources Evaluation Series No 5. Springer, Cham p. 861.
- Mamou, A. (1994). Impact of the artificial recharge on the groundwater flow system of Mornag using canal Medjerda Cap Bon water [Impact de la recharge artificielle par les eaux du canal Mejerda Cap Bon sur le système aquifère de Mornag]. Technical Report, DGRE, Tunis, 39p.
- Mays, L. W. (2013). Groundwater resources sustainability: Past, present, and future. *Water Resources Management*, 27(13), 4409–4424.
- McInnis, D., Silliman, S., Boukari, M., Yalo, N., Orou-Pete, S., Fertenbaugh, C., Sarre, K., & Fayomi, H. (2013). Combined application of electrical resistivity and shallow groundwater sampling to assess salinity in a shallow coastal aquifer in Benin, West Africa. *Journal of Hydrology*, 505, 335–345.
- McLean, W., Jankowski, J., & Lavitt, N. (2000). Groundwater quality and sustainability in an alluvial aquifer, Australia. In Proceedings of the 30th IAH congress on groundwater: “Groundwater: Past achievements and future challenges”. Cape Town, South Africa, 2000-11-26 (pp. 567–573).
- Mejri, S., Chekirbane, A., Tsujimura, M., Boughdiri, M., & Mlayah, A. (2018). Tracing groundwater salinization processes in an inland aquifer: A hydrogeochemical and isotopic approach in Sminja aquifer (Zaghouan, northeast of Tunisia). *Journal of African Earth Sciences*, 147, 511–522.
- Merhebene, H. (1998). Piezometric database of the groundwater flow system of Mornag plain [Etablissement de la banque de données piézométriques du système aquifère de la plaine de Mornag]. Technical Report, DGRE, Tunis, 58p.
- Milly, P. C., Dunne, K. A., & Vecchia, A. V. (2005). Global pattern of trends in streamflow and water availability in a changing climate. *Nature*, 438(7066), 347–350.
- Mishra, A. K., Deep, S., & Choudhary, A. (2015). Identification of suitable sites for organic farming using AHP & GIS. *The Egyptian Journal of Remote Sensing and Space Science*, 18(2), 181–193.
- Mlayah, A., Ferreira Da Silva, E., Hatira, N., Jellali, S., Lachaal, F., Charef, A., Noronha, F., & Ben Hamza, C. (2011). Bassin d'oued Serrat: Terrils et rejets domestiques, reconnaissance des métaux lourds et polluants, impact sur les eaux souterraines (nord-ouest de la Tunisie). *Revue Des Sciences De L'eau/Journal of Water Science*, 24(2), 159–175.
- Morsy, K. M., Morsy, A. M., & Hassan, A. E. (2018). Groundwater sustainability: Opportunity out of threat. *Groundwater for Sustainable Development*, 7, 277–285.
- Moussa, A. B., Chandoul, S., Mzali, H., Salem, S. B. H., Elmejri, H., Zouari, K., Hafiane, A., & Mrabet, H. (2020). Hydrogeochemistry and evaluation of groundwater suitability for irrigation purpose in the Mornag region, northeastern Tunisia. *Environment, Development and Sustainability*, 23(2), 2698–2718.
- Naudet, V., Revil, A., Rizzo, E., Bottero, J. Y., & Bégassat, P. (2004). Groundwater redox conditions and conductivity in a contaminant plume from geoelectrical investigations. *Hydrology and Earth System Sciences*, 8(1), 8–22.
- Nayeri, M., Hosseini, S. A., Javadi, S., & Sharafati, A. (2021). Spatial differentiation characteristics of groundwater stress index and its relation to land use and subsidence in the Varamin Plain, Iran. *Natural Resources Research*, 30(1), 339–357.
- Piper, A. M. (1944). A graphic procedure in the geochemical interpretation of water analysis. *Transactions of the American Geophysical Union*, 25, 914–923.
- Praveena, S. M., Abdullah, M. H., Bidin, K., & Aris, A. Z. (2012). Sustainable groundwater management on the small island of

- Manukan, Malaysia. *Environmental Earth Sciences*, 66(3), 719–728.
- Ranjan, R. (2012). Natural resource sustainability versus livelihood resilience: Model of groundwater exploitation strategies in developing regions. *Journal of Water Resources Planning and Management*, 138(5), 512–522.
- Rekaya, M., (1987). Update of the hydrogeological context of Mornag plain [Actualisation du contexte hydrogéologique de la plaine de Mornag]. Technical Report, DGRE, Tunis, 18p.
- Rengasamy, P., & Olsson, K. A. (1993). Irrigation and sodicity. *Soil Research*, 31(6), 821–837.
- Rhoades, J. D., Krueger, D. B., & Reed, M. J. (1968). The effect of soil-mineral weathering on the sodium hazard of irrigation waters. *Soil Science Society of America Journal*, 32(5), 643–647.
- Richards, L. A. (1954). Diagnosis and improvement of saline and alkali soils. LWW. 78(2), 154.
- Rozanski, K., Araguás-Araguás, L., & Gonfiantini, R. (1993). Isotopic patterns in modern global precipitation. *GMS*, 78, 1–36.
- Saaty, T. L. (2000). *Fundamentals of decision making and priority theory with the analytic hierarchy process* (Vol. 6). RWS publications.
- Saaty, T. L. (2005). *Theory and applications of the analytic network process: Decision making with benefits, opportunities, costs, and risks*. RWS publications.
- Scanlon, B. R., Healy, R. W., & Cook, P. G. (2002). Choosing appropriate techniques for quantifying groundwater recharge. *Hydrogeology Journal*, 10(1), 18–39.
- Scanlon, B. R., Keese, K. E., Flint, A. L., Flint, L. E., Gaye, C. B., Edmunds, W. M., & Simmers, I. (2006). Global synthesis of groundwater recharge in semiarid and arid regions. *Hydrological Processes: An International Journal*, 20(15), 3335–3370.
- Schlesinger, W. H., Reynolds, J. F., Cunningham, G. L., Huenneke, L. F., Jarrell, W. M., Virginia, R. A., & Whitford, W. G. (1990). Biological feedbacks in global desertification. *Science*, 247(4946), 1043–1048.
- Schoups, G., Addams, C. L., Minjares, J. L., & Gorelick, S. M. (2006). Sustainable conjunctive water management in irrigated agriculture: Model formulation and application to the Yaqui Valley, Mexico. *Water Resources Research*, 42, W10417. <https://doi.org/10.1029/2006WR004922>.
- Singha, K., & Gorelick, S. M. (2005). Saline tracer visualized with three-dimensional electrical resistivity tomography: Field-scale spatial moment analysis. *Water Resources Research*, 41(5), W05023. <https://doi.org/10.1029/2004WR003460>.
- Soussi, M., Mangold, C., Enay, R., Boughdiri, M., & Ben Ismail, M. H. (2000). Le Jurassique inférieur et moyen de la Tunisie septentrionale; corrélations avec l'Axe Nord-Sud et paléogéographie. *Geobios*, 33, 437–446.
- Stimson, J., Frape, S., Drimmie, R., & Rudolph, D. (2001). Isotopic and geochemical evidence of regional-scale anisotropy and interconnectivity of an alluvial fan system, Cochabamba Valley Bolivia. *Applied Geochemistry*, 16(9–10), 1097–1114.
- Todd, D. K., & Mays, L. W. (2004). *Groundwater hydrology*. JoWiley & Sons.
- Turki, M. M. (1985). Polycinématique et contrôle sédimentaire associé sur la cicatrice Zaghouan-Nebhana. Doctoral dissertation. University of Tunis El Manar, 262 p.
- Vadiati, M., Adamowski, J., & Beynaghi, A. (2018). A brief overview of trends in groundwater research: Progress towards sustainability. *Journal of Environmental Management*, 223, 849–851.
- Wilcox, L. V. (1948). The quality of water for irrigation use (No. 1488–2016–124600).
- Wilcox, L. (1955). Classification and use of irrigation waters (No. 969). US Department of Agriculture.
- Zaman, M., Shahid, S. A., & Heng, L. (2018). Irrigation water quality. *Guideline for salinity assessment, mitigation and adaptation using nuclear and related techniques* (pp. 113–131). Cham: Springer.
- Zaree, M., Javadi, S., & Neshat, A. (2019). Potential detection of water resources in karst formations using APLIS model and modification with AHP and TOPSIS. *Journal of Earth System Science*, 128(4), 1–12.
- Zouari, K., Aranyosy, J. F., Mamou, A., & Fontes, J. C. (1985). Etude isotopique et géochimique des mouvements et de l'évolution des solutions de la zone aérée des sols sous climat semi-aride (Sud tunisien). *Stable and Radioactive Isotopes in the Study of the Unsaturated Soil Zone, IAEA-TECDOC*, 357, 121–143.
- Zume, J. T., & Tarhule, A. A. (2011). Modelling the response of an alluvial aquifer to anthropogenic and recharge stresses in the United States Southern Great Plains. *Journal of Earth System Science*, 120(4), 557–572.